Acta Crystallographica Section D
Biological Crystallography
ISSN 0907-4449

The structure of apo tryptophanase from *Escherichia coli* reveals a wide-open conformation

Natalia Tsesin,[a]‡ Anna Kogan,[a]‡ Garik Y. Gdalevsky,[a] Juha-Pekka Himanen,[b] Rivka Cohen-Luria,[a] Abraham H. Parola,[a] Yehuda Goldgur[a,b] and Orna Almog[c]*

[a]Department of Chemistry, Ben-Gurion University of the Negev, POB 653, Beer-Sheva 84105, Israel, [b]Structural Biology Program, Memorial Sloan-Kettering Cancer Center, 1275 York Avenue, New York, NY 10021, USA, and [c]Department of Clinical Biochemistry, Ben-Gurion University of the Negev, POB 653, Beer-Sheva 84105, Israel

‡ These authors contributed equally to the paper.

Correspondence e-mail: almogo@bgu.ac.il

Received 20 June 2007
Accepted 24 July 2007

PDB Reference: apo tryptophanase, 2oqx, r2oqxsf.

The crystal structure of apo tryptophanase from *Escherichia coli* (space group *F*222, unit-cell parameters $a = 118.4$, $b = 120.1$, $c = 171.2$ Å) was determined at 1.9 Å resolution using the molecular-replacement method and refined to an *R* factor of 20.3% (R_{free} = 23.2%). The structure revealed a significant shift in the relative orientation of the domains compared with both the holo form of *Proteus vulgaris* tryptophanase and with another crystal structure of apo *E. coli* tryptophanase, reflecting the internal flexibility of the molecule. Domain shifts were previously observed in tryptophanase and in the closely related enzyme tyrosine phenol-lyase, with the holo form found in an open conformation and the apo form in either an open or a closed conformation. Here, a wide-open conformation of the apo form of tryptophanase is reported. A conformational change is also observed in loop 297–303. The structure contains a hydrated Mg^{2+} at the cation-binding site and a Cl^- ion at the subunit interface. The enzyme activity depends on the nature of the bound cation, with smaller ions serving as inhibitors. It is hypothesized that this effect arises from variations of the coordination geometry of the bound cation.

1. Introduction

Tryptophanase (tryptophan indole-lyase; EC 4.1.99.1; Trpase) is a widely distributed bacterial pyridoxal phosphate-dependent enzyme that catalyzes α,β-elimination and β-replacement of L-tryptophan and a variety of other β-substituted L-amino acids (Snell, 1975). The decomposition of tryptophan produces indole together with ammonia and pyruvate. Indole has recently been shown to act as a cell-to-cell signaling molecule, leading to biofilm formation in various species of bacteria (Wang *et al.*, 2001; Martino *et al.*, 2003; Mueller *et al.*, 2007). Therefore, Trpase might serve as a target for a new generation of potential antibiotics. It has recently been reported that indole signaling plays an important role in the stable maintenance of multicopy plasmids (Chant & Summers, 2007). In addition, Trpase was shown to be capable of binding Rcd, a short RNA molecule involved in the resolution of plasmid multimers. Binding of Rcd increases the affinity of Trpase for tryptophan, suggesting that Trpase serves as a multifunctional enzyme (Chant & Summers, 2007). Trpase consists of four identical subunits. Each monomer binds one molecule of the cofactor pyridoxal phosphate (PLP), which forms an aldimine bond with a Lys270 residue adjacent to the active site. The enzyme requires monovalent cations (K^+, NH_4^+, Tl^+) for its activity (Suelter & Snell, 1977). The subunit molecular weight of Trpase from *Escherichia coli* is 52.8 kDa. Although

Table 1
Diffraction data and model-refinement statistics.

Values in parentheses are for the highest resolution shell.

Resolution range (Å)	15–1.9 (1.97–1.90)
R_{merge}	0.07 (0.31)
Completeness (%)	95.4 (99.3)
Average redundancy	3.3 (3.2)
$\langle I\rangle/\langle\sigma(I)\rangle$	42.54 (4.25)
R_{cryst} (%)	20.3 (26.1)
No. of reflections in refinement	88583
R_{free} (%)	23.2 (28.6)
No. of reflections used for R_{free}	2631 (419)
No. of protein atoms	3670
No. of water molecules	364
Average *B* factor for protein atoms (Å^2)	27.0
R.m.s. deviations from ideality	
Bond lengths (Å)	0.005
Bond angles (°)	1.20
B-factor correlation (Å^2)	
Main-chain bond	1.090
Main-chain angle	1.610
Side-chain bond	1.930
Side-chain angle	2.760
Ramachandran analysis (%)	
Most favored	91.0
Additionally allowed	8.5
Generously allowed	0.5

biochemical studies of *E. coli* Trpase have been carried out for many years, X-ray structural investigations had been unsuccessful owing to difficulties in obtaining well diffracting crystals. The first crystals of *E. coli* Trpase were obtained as early as 1965 (Newton *et al.*, 1965). The first crystals of the *E. coli* enzyme suitable for X-ray analysis were reported in 1991 (Kawata *et al.*, 1991) and were improved in 1994 (Dementieva *et al.*, 1994). We have previously described the crystallization of the apo form of *E. coli* Trpase along with W330F and Y74F mutants (Kogan *et al.*, 2004). The crystal structure of Trpase from *Proteus vulgaris*, which shares 51% identity and greater than 60% similarity with the *E. coli* enzyme, has been reported (Isupov *et al.*, 1998). A 2.8 Å structure of *E. coli* Trpase has recently been published (Ku *et al.*, 2006; referred to here as the apoI structure). Since most kinetic and mechanistic studies have been performed on the Trpase from *E. coli*, there is a need for a high-resolution crystal structure of this enzyme. Here, we present the crystal structure of wild-type apo Trpase from *E. coli* (referred to here as the apoII structure) refined at 1.9 Å resolution.

2. Materials and methods

2.1. Protein purification, crystallization and data collection

E. coli apo Trpase was purified, assayed and crystallized as described previously (Kogan *et al.*, 2004). Crystallization was carried out by the hanging-drop vapor-diffusion method. The protein at 30–50 mg ml^{-1} in 0.05 *M* Tris, 0.1 *M* KCl pH 7.5, 2 m*M* EDTA and 5 m*M* 2-mercaptoethanol was mixed with precipitant solution containing 30%(*w*/*v*) PEG 400, 100 m*M* HEPES pH 7.5, 200 m*M* $MgCl_2$, 5 m*M* 2-mercaptoethanol in a 3:2 ratio. Prior to freezing, crystals were transferred to Paratone oil (Hampton Research) and excess liquid was removed. A data set was collected at 100 K using a Rigaku RU-H3R rotating-anode generator and a MAR345 image-plate detector. Flash-freezing was performed in liquid nitrogen. Data were processed and scaled using the *DENZO*/*SCALEPACK* program package (Otwinowski & Minor, 1997). Crystals belong to space group *F*222, with unit-cell parameters $a = 118.4$, $b = 120.3$, $c = 171.3$ Å. The asymmetric unit contains a monomer with molecular weight 52 kDa, giving a specific volume of 2.9 Å^3 Da^{-1} and a solvent content of 58% (Matthews, 1968). Data-collection statistics are presented in Table 1.

2.2. Structure determination and refinement

Attempts to solve the structure by the molecular-replacement method using the program *AMoRe* (Navaza, 1994) with *E. coli* holo Trpase (our unpublished data) or *P. vulgaris* Trpase (Isupov *et al.*, 1998) as a search model failed. The phase problem was solved utilizing the fact that the tetrameric molecule has three perpendicular symmetry axes (point group 222). Since the crystallographic symmetry is *F*222 with a monomer in the asymmetric unit, the molecular symmetry axes should coincide with the crystallographic dyads. The monomer possesses an elongated shape, implying that the longest molecular dimension should lie along the long crystallographic axis. This leaves only two possibilities for the orientation of the molecule. Both were checked by rigid-body refinement in *CNS* (Brünger, 1992). One of the possible orientations led to the correct placement of the large domain (see structure description). The small domain was built into difference electron-density maps. The structure was refined using the simulated-annealing and position-refinement protocols of *CNS*. Manual corrections to the model were carried out with the graphics program *O* (Jones *et al.*, 1991). The final model contains residues 5–100 and 103–471 of Trpase (3760 protein atoms), one magnesium ion, one chloride ion located on a twofold crystallographic axis, one HEPES molecule and 364 water molecules. Two cysteines, Cys298 and Cys352, are found in an oxidized form, forming disulfide bonds with 2-mercaptoethanol molecules. The final *R* factor is 20.3% for all data in the resolution range 15–1.9 Å (R_{free} = 23.2%). Of the nonglycine residues, 91.0% fall in the most favored regions of a Ramachandran plot (Ramakrishnan & Ramachandran, 1965) generated by *PROCHECK* (Laskowski *et al.*, 1993). The refinement statistics are summarized in Table 1.

3. Results and discussion

3.1. Overall structure

As might be expected from the high sequence homology between the Trpases from *P. vulgaris* and *E. coli*, both enzymes share the same fold consisting of two domains: large and small. However, structural alignment of the holo Trpase from *P. vulgaris* and two structures of Trpase from *E. coli* [apoII Trpase (this structure) and apoI Trpase (Ku *et al.*, 2006)] revealed significant differences in the relative orientation of the two domains. The conformational change arises

from bending of the loops between strands βI and βY and helices α11 and α12 (secondary-structure element numbering according to Isupov *et al.*, 1998) that form links between the large and the small domains. The domains themselves essentially move like rigid bodies. The r.m.s.d. for 465 C^{α} atoms of the two superimposed structures of *E. coli* Trpase is 3.4 Å and those for the large and small domains separately are 0.65 and 0.99 Å, respectively. The two structures of *E. coli* Trpase are observed in the most open and closed states, while *P. vulgaris* holo Trpase is found in an intermediate state (Fig. 1). As a result, the distance between the corresponding C^{α} atoms in the small domain of the two apo structures reaches 14.5 Å when the large domains are superimposed. Since both enzymes share the same substrate and the same catalytic mechanism, it is reasonable to assume that the observed deviations result from external factors (enzyme state, pH and crystal packing) rather than from sequence variations and reflect the intrinsic flexibility of the molecule. The active site of *P. vulgaris* holo Trpase contains a PLP molecule covalently attached to the catalytic lysine. In the apoI structure, a sulfate ion is found in a position overlapping with the phosphate moiety of PLP, as seen in the structure of the holo enzyme. In the apoII structure, a HEPES molecule, present in the crystallization buffer, is bound in the active site. Its sulfonyl moiety is shifted with respect to the phosphate and the sulfate in the other two structures by approximately 6 Å. However, the pattern of interactions with the protein is similar: HEPES is found in the vicinity of Lys270, Thr52 and Arg419. It is extremely unlikely that the binding of chemically similar moieties (phosphate, sulfate and sulfonyl groups) would induce opposing effects on the molecule. Open and closed conformation structures have also been found in tyrosine phenol-lyase (TPL). In this case, the conformational change also results from a movement of the small domain (Milić *et al.*, 2006). In TPL, one of the subunits of the apo enzyme is found in a closed conformation, causing the catalytic cleft to disappear. The apoII structure is thus the first member of this enzyme family to have the apo form in an open conformation. The transition between the open and closed conformation of apo TPL was attributed to the difference in pH of the crystallization mixture (6.0 compared with 8.0). This is unlikely to be the case for the Trpases, since all three were crystallized at similar pH (holo, 7.8; apoI, 7.9; apoII, 7.5), suggesting that various conformations of Trpase exist in the same pH range. Superposition of the two observed conformations of apo TPL on the apoI and apoII structures of Trpase reveals that the open and the closed conformations of apo TPL are remarkably close to the corresponding conformations of apo Trpase, raising the possibility that both enzymes have several conformations that are preferred among the continuum of possible states.

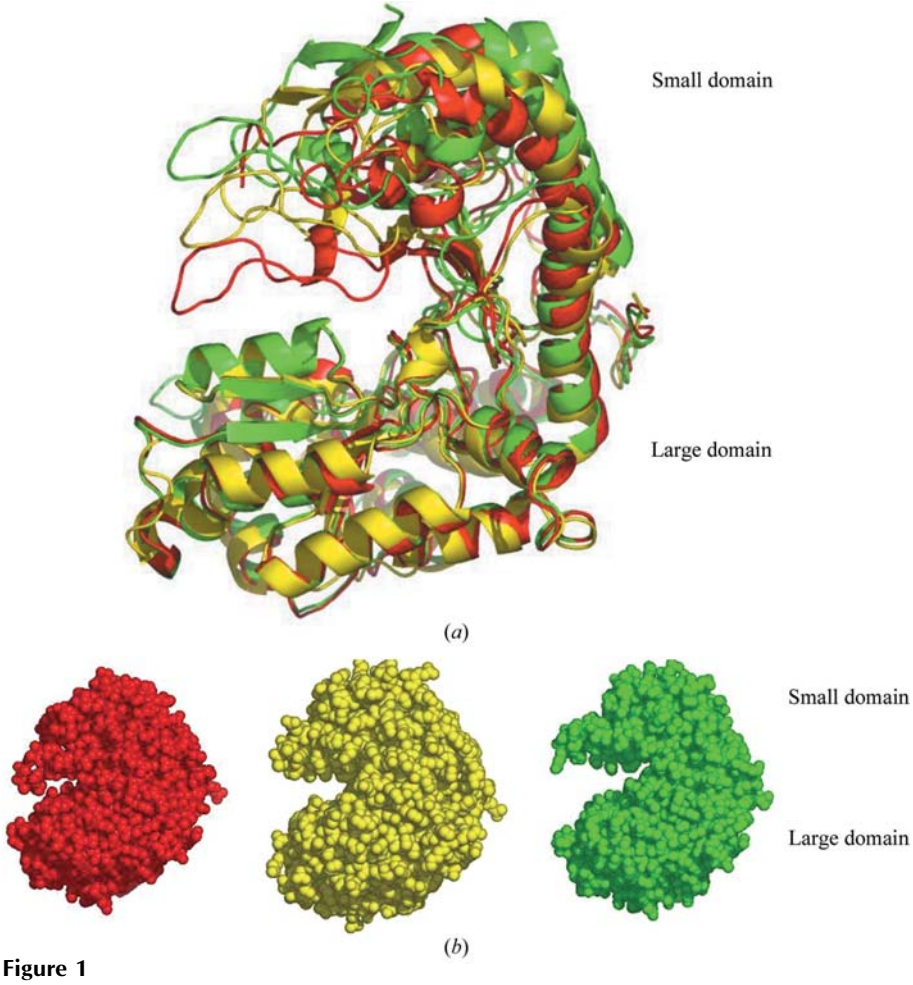

Figure 1
(*a*) Superposition of Trpase monomers from *P. vulgaris* (holo form, shown in yellow) and *E. coli* (apoI structure, red; apoII structure, green) shown as ribbons. The apoI structure is found in the most closed conformation, while the apoII structure is the most open. (*b*) Space-filling models of the three structures, showing the variations in the catalytic cleft width.

Several regions of the apoII Trpase crystal structure also deviate in conformation from those of the holo and apoI structures. As pointed out by Ku *et al.* (2006), residues 122–128 and 283–288 differ in the apoI and holo structures. Since the conformation of these residues in the apoI and apoII structures is virtually identical, these variations should be attributed to relatively low sequence homology between the *P. vulgaris* and *E. coli* enzymes in these regions.

Another significant difference is observed in the conformation of region 292–307 (Fig. 2). In the holo form of the enzyme, this stretch comprises the C-terminal part of helix α10 and a β-turn. In the apoII structure, it lacks regular secondary structure. This region is located at the entrance to the catalytic cleft, at a distance of 18 Å from the active site. The observed conformation

of the loop is stabilized by a hydrogen bond formed between the carbonyl O atom of Leu306 and a water molecule coordinating the Mg^{2+} ion (see §3.4). The exact cause of this conformational difference is not clear. It could arise from the oxidation of Cys298, which is located within this loop, or from the binding of a magnesium cation.

3.2. Molecular association

The tetrameric quaternary structure of the enzyme is maintained by the interface formed by a four-helix bundle of helices α2 from each subunit. In *P. vulgaris*, the side chains of Trp62 and Ile66 belonging to these helices form a hydrophobic cluster at the center of the tetramer. In *E. coli*, the structural equivalents are Gln64 and Met68, which renders the core much less hydrophobic. The hydrophobic interactions of tryptophans are substituted by the two hydrogen bonds between the glutamines. Amazingly, despite the lack of sequence homology in the region, the positions of C^{α} atoms superimpose very well (the r.m.s.d. of the four-helix bundle is 0.1 Å). The side chains of Met68 are found in two alternative conformations.

Additional stabilization of the tetrameric interface is achieved by the binding of a chloride ion between two side chains of Arg69 residues belonging to two adjacent subunits of the noncatalytic dimer. The peaks in the electron density were interpreted as corresponding to Cl^- based on their intensity, anomalous scattering and chemical environment (Fig. 3). The Cl^- ions are located on a crystallographic twofold axis, meaning that two of them are bound in the tetramer. The presence of anions at the intersubunit interface indicates that the stability of the noncatalytic interface might depend on the nature and the concentration of anions. In the absence of a suitable anion, electrostatic repulsion between the side chains will presumably lower the stability of association. On the other hand, since the total charge of the two arginines to which Cl^- is bound amounts to +2, binding of a polyvalent anion (such as HPO_4^{2-} or SO_4^{2-}) at the same site should stabilize the noncatalytic dimer further. It has been observed that cold inactivation of *E. coli* Trpase, which is attributed to the dissociation of the enzyme into dimers at low temperatures, is affected by the ionic strength and the ion composition of the buffer (Erez *et al.*, 1998). The interpretation of these results

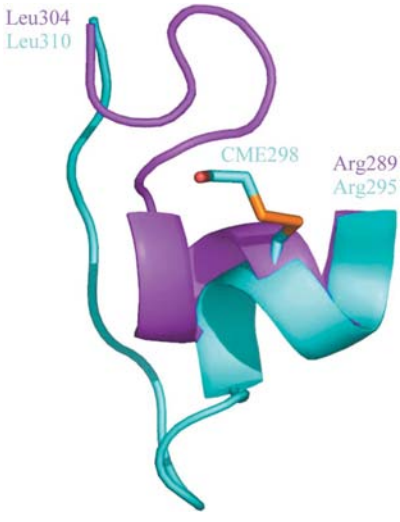

Figure 2
Loop 292–307. The conformation observed for the holo form is shown in magenta, which is nearly identical to the apoI crystal form. The same loop in the apoII structure is colored cyan. Cys298 forms a disulfide bond with a 2-mercaptoethanol molecule present in the crystallization mixture.

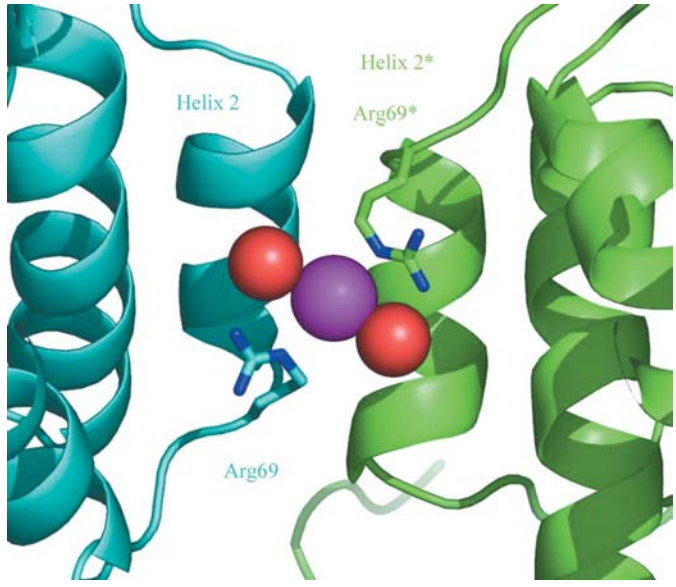

Figure 3
The binding of chloride ion at the subunit interface. The view is along the crystallographic twofold axis: symmetry-related subunits are shown in cyan and green. The Cl^- ion is colored magenta; the red spheres represent the coordinating water molecules.

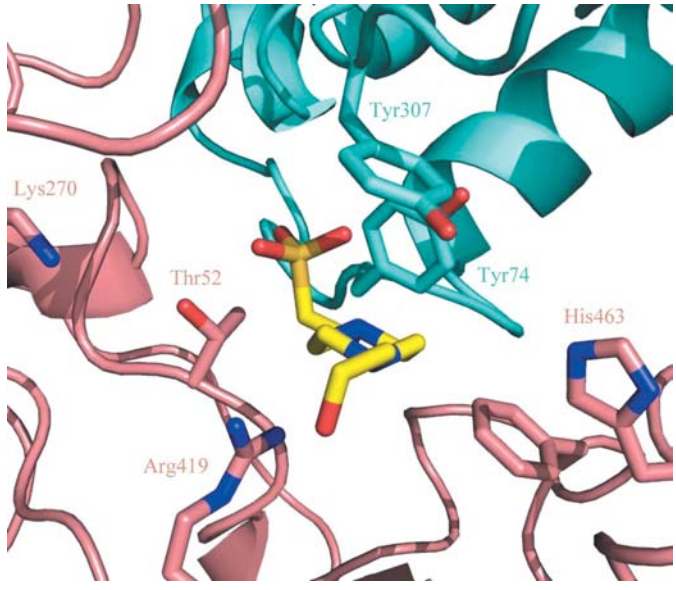

Figure 4
HEPES molecule in the active site. Two symmetry-related subunits are shown in pink and cyan. Thr52, Tyr74 and Tyr307 (both from the symmetry-related subunit) interact with the HEPES molecule, while the catalytic Lys270 as well as Arg419 and His463, which are important for substrate binding, are shown for reference.

might need to take into account possible dissociation along the interface of the noncatalytic dimer.

3.3. Active site

The amino-acid sequence in the active site is strongly conserved between the *P. vulgaris* and *E. coli* Trpases. However, the active-site conformation appears to differ significantly in the three Trpase structures. These differences arise from the global domain shift discussed above and the binding of the PLP cofactor and other molecules at the active site. While the geometry of the PLP-binding site remains intact, the residues believed to participate in tryptophan substrate binding, namely Arg419 and His463 (Demidkina *et al.*, 2003), are shifted significantly from their positions in the other Trpase structures. It is likely that Trpase in the wide-open conformation is incapable of binding tryptophan owing to the distortion in the substrate-binding site. This assumption is supported by the observation that no electron density for tryptophan was found in apoII crystals soaked in a solution containing 100 m*M* tryptophan. In the crystal form reported here, an extended electron density was found in the active site of the enzyme which could not be attributed to the protein. Judging by its shape, we assume that a HEPES molecule is bound in the active site (Fig. 4).

3.4. Cation binding and activity

Monovalent cations are required for the activity of Trpase. While K^+, NH_4^+, Tl^+ and Rb^+ are known to accelerate the enzymatic reaction, Li^+ and Na^+ serve as inhibitors (Snell, 1975). The cation-binding site is well conserved both in sequence and structure in the *E. coli* and *P. vulgaris* enzymes. Potassium ion was found bound to both holo Trpase from *P. vulgaris* and the apoI structure and was coordinated by the side chain of Glu72, the main-chain carbonyls of Gly55 and Pro275 (numbering according to the sequence of *E. coli* Trpase) and three water molecules. To our surprise, despite the fact that the crystallization mixture contained 50 m*M* K^+, the cation-binding site appeared to be occupied by an octahedral structure with a strong peak in the middle (Fig. 5). The distance between the central peak and each of the vertices was between 1.9 and 2.1 Å. The octahedron apparently represents a solvated cation which cannot be interpreted as a K^+ ion because of the short distances to the solvating water molecules. Since our buffer contained Mg^{2+}, it is reasonable to attribute the observed electron density to a solvated Mg^{2+}. The protein residues of the cation-binding site, together with three water molecules, form the second coordination shell. This result suggests that the specificity of the cation-binding site is low and that various ions can compete for binding. This provides a plausible explanation of the observed dependence of Trpase activity on the nature of the cation. Thus, small cations (Li^+, Na^+ and Mg^{2+}) bind to Trpase in the solvated form, while larger cations (K^+, NH_4^+, Tl^+ and Rb^+) lose their solvation shell upon binding. It is hereby hypothesized that only naked ions are capable of activating Trpase. To support this conclusion, we measured the enzyme activity in the presence of K^+ (for reference), of Mg^{2+} and of both. In the absence of K^+ only trace activity was observed, while in a 1:4 mixture of K^+ and Mg^{2+} Trpase activity was reduced by 50%, indicating that both cations compete for binding on Trpase.

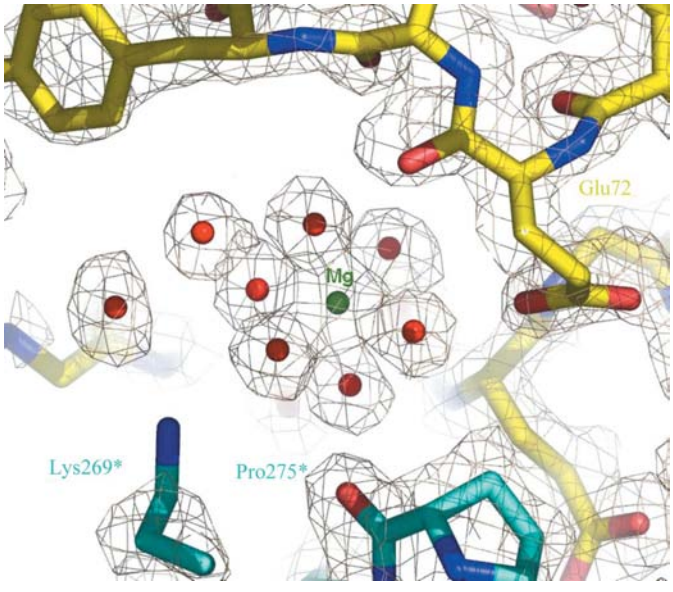

Figure 5
Cation-binding site. Electron density shows the octahedral coordination of the metal ion, which makes no direct contacts with the protein. Residues belonging to two adjacent subunits and forming the second coordination shell are shown.

4. Conclusions

The crystal structure of the apo form of *E. coli* tryptophanase was determined at 1.9 Å resolution from a new crystal form. The structure demonstrates significant variations in the enzyme conformation compared with other tryptophanase structures, suggesting that the enzyme molecule is flexible. This flexibility might account for the relatively low substrate specificity and needs to be taken into account in structure-based inhibitor design. The tetrameric structure is stabilized by a chloride ion bound at the subunit interface, explaining the dependency of the stability of the enzyme to cold inactivation on the ionic strength and the composition of the buffer. The cation-binding site is occupied by a hydrated magnesium ion, which inhibits the enzyme activity, indicating that the affinity of the enzyme for the potassium cofactor and the magnesium inhibitor is similar. Two cysteines are found to form disulfide bonds with 2-mercaptoethanol.

We are most grateful to Professor Robert S. Phillips of the Chemistry and Biochemistry Department of the University of Georgia, Athens, Georgia for providing us with the Trpase plasmid.

References

Brünger, A. T. (1992). *Nature (London)*, **355**, 472–474.
Chant, E. L. & Summers, D. K. (2007). *Mol. Microbiol.* **63**, 35–43.

Dementieva, I. S., Zakomirdina, L. N., Sinitzina, N. I., Antson, A. A., Wilson, K. S., Isupov, M. N., Lebedev, A. A. & Harutyunyan, E. H. (1994). *J. Mol. Biol.* **235**, 783–785.
Demidkina, T. V., Zakomyrdina, L. N., Kulikava, V. V., Dementieva, I. S., Faleev, N. G., Ronda, L., Mozzarelli, A., Gollnick, P. D. & Phillips, R. S. (2003). *Biochemistry*, **42**, 11161–11169.
Erez, T., Gdalevsky, G. Y., Torchinsky, Y. M., Phillips, R. S. & Parola, A. H. (1998). *Biochim. Biophys. Acta*, **1384**, 365–372.
Isupov, M. N., Antson, A. A., Dodson, G. G., Dementieva, I. S., Zakomirdina, L. N., Wilson, K. S., Dauter, Z., Lebedev, A. A. & Harutyunyan, E. H. (1998). *J. Mol. Biol.* **276**, 603–623.
Jones, T. A., Zou, J.-Y., Cowan, S. W. & Kjeldgaard, M. (1991). *Acta Cryst.* A**47**, 110–119.
Kawata, Y., Tani, S., Sato, M., Katsube, Y. & Tokushige, M. (1991). *FEBS Lett.* **284**, 270–272.
Kogan, A., Gdalevsky, G. Y., Cohen-Luria, R., Parola, A. H. & Goldgur, Y. (2004). *Acta Cryst.* D**60**, 2073–2075.
Ku, S.-Y., Yip, P. & Howell, P. L. (2006). *Acta Cryst.* D**62**, 814–823.
Laskowski, R. A., MacArthur, M. W., Moss, D. S. & Thornton, J. M. (1993). *J. Appl. Cryst.* **26**, 283–291.
Martino, P. D., Fursy, R., Bret, L., Sundararaju, B. & Phillips, R. S. (2003). *Can. J. Microbiol.* **49**, 443–449.
Matthews, B. W. (1968). *J. Mol. Biol.* **33**, 491–497.
Milić, D., Matkovic Calogovic, D., Demidkina, T. V., Kulikova, V. V., Sunitzina, N. I. & Antson, A. A. (2006). *Biochemistry*, **45**, 7544–7522.
Mueller, R. S., McDougald, D., Cusumano, D., Sodhi, N., Kjelleberg, S., Azam, F. & Bartlett, D. H. (2007). *J. Bacteriol.* **189**, 5348–5360.
Navaza, J. (1994). *Acta Cryst.* A**50**, 157–163.
Newton, W. A., Morino, Y. & Snell, E. E. (1965). *J. Biol. Chem.* **240**, 1211–1218.
Otwinowski, Z. & Minor, W. (1997). *Methods Enzymol.* **276**, 307–326.
Ramakrishnan, C. & Ramachandran, G. N. (1965). *Biophys. J.* **5**, 909–933.
Snell, E. E. (1975). *Adv. Enzymol.* **42**, 287–332.
Suelter, C. H. & Snell, E. E. (1977). *J. Biol. Chem.* **252**, 1852–1857.
Wang, D., Ding, X. & Rather, P. N. (2001). *J. Bacteriol.* **183**, 4210–4216.